Journal of Agrometeorology

(A publication of Association of Agrometeorologists)

ISSN : 0972-1665 (print), 2583-2980 (online)

Vol. No. 28 (1) : 71 - 79 (March - 2026)

https://doi.org/10.54386/jam.v28i1.3285

https://journal.agrimetassociation.org/index.php/jam

Research paper

Validation of a simple MODIS Land Surface Temperature-Based model for potential Evapotranspiration (PET) using long-term Global Dataset

MOHAMMED EL-SHIRBENY[1,2]

[1]*National Authority for Remote Sensing and Space Sciences (NARSS), Cairo, Egypt,*

[2]*National Center for Vegetation Cover Development and Combating Desertification (NCVC), Riyadh, Saudi Arabia.*

Email: m.elshirbeny@narss.sci.eg; melshirbeny@ncvc.gov.sa

ABSTRACT

Accurate and usable potential evapotranspiration (PET) estimation is important for managing water resources around the world, planning agriculture, and adapting to climate change. Complex energy balance models yield valuable insights; yet practical applications necessitate straightforward, resilient, and simply implementable long-term monitoring methodologies. This study confirms a more straightforward empirical model that estimates monthly PET only utilizing MODIS land surface temperature (LST) data of 25 years (2000–2024), addressing a deficiency in the comprehension of simple model transferability across global climatic regimes. The LST products (MOD11A1/MYD11A1) processed in Google Earth Engine to confirm the accuracy of PET predictions against the FAO-56 Penman–Monteith (FAO-PM) technique, which was based on data from 58 ground-based meteorological stations in 5 Major Köppen–Geiger climate zones. The model was very accurate ($R^2 = 0.76$, RMSE = 30.02 mm/month); however, it was completely unique in different areas because of environmental controls. The model worked well in the Continental and Mediterranean climate zones ($R^2 = 0.93$, NSE = 0.88), but it had trouble in the Tropical Wet ($R^2 = 0.39$, NSE = -6.15) and Polar ($R^2 = 0.64$, NSE = -2.64) regions because of the moisture in the air and the complicated way energy is divided. The initial comprehensive analysis of basic LST-based model constraints sets essential standards for operational implementation and underscores the necessity for climate-zone-specific parameterization in this global, long-term validation. The results enhance the comprehension of environmental influences on remote sensing-derived PET estimation and inform water resource management in a dynamic climate.

Keywords: Potential evapotranspiration (PET), MODIS LST, FAO Penman–Monteith, Global validation, Climate zones, Remote sensing, Google earth engine (GEE)

The potential evapotranspiration (PET) is a crucial hydrological indicator that illustrates the maximum atmospheric moisture demand from a vegetated area with unlimited soil water availability (El-Shirbeny *et al.,* 2021, 2022; Pimentel *et al.,* 2023; Afify *et al.,* 2023). The precision of PET estimates is crucial for various applications, including irrigation management, agricultural water distribution, drought monitoring, and the simulation of terrestrial hydrological processes in the context of climate change (Zhou & Yu, 2024). The FAO-PM equation is the standard for PET calculations because it is based on strong physical principles and includes all the important meteorological factors (El-Shirbeny *et al.,* 2016). However, the practical implementation of the FAO-PM approach is hindered by its high data requirements (Faseyiku *et al.,* 2024). This methodology's reliance on a range of high-frequency meteorological factors, such as solar radiation, temperature, humidity, and wind speed, can be impractical in many regions where ground-based observational networks are either sparse or nonexistent (Peng *et al.,* 2024). Such data limitations create significant challenges for consistent water resource assessments, particularly in remote, economically developing, and data-deficient areas.

Recently, data-driven approaches have increasingly been used to estimate PET in data-scarce or meteorologically complex regions (Caguiat *et al.,* 2025). Accurate estimation of crop water

Article info - DOI: *https://doi.org/10.54386/jam.v28i1.3285*

Received:01 February 2025; Accepted: 30 December 2025; Published online : 1 March 2026

requirements is still essential for sustainable management of agricultural water resources; ET is the main indicator used to evaluate this need (Salam & Al Mazrooe, 2006; Mehta & Pandey, 2016). There are large uncertainties regarding data limitations, model assumptions, and scale mismatches across different techniques for estimating ET. This situation emphasizes the importance of validating within-the-context and integrating artificial intelligence with process-based and remote sensing approaches (Ezenne *et al.,* 2023; Singh *et al.,* 2023).

Satellite remote sensing for spatially continuous and coherent terrestrial surface variable monitoring is a promising answer to this essential challenge. The land surface temperature (LST) is a key remote sensing measure for surface energy exchanges. LST is a good proxy for ET and PET because it shows the balance between surface energy inputs and outputs and has a strong inverse association with evaporative cooling. This underlying link has inspired a variety of LST-based models, from complicated surface energy balance frameworks needing many distant sensing inputs to simpler empirical equations that directly use the LST-PET association (Afify *et al.,* 2023; Danodia *et al.,* 2024). Their operational utility for large monitoring initiatives makes these simplified empirical models appealing. Their computational efficiency, low input datasets, and high scalability make them ideal for constructing large, long-term worldwide PET datasets where meteorological measurements are limited.

These simplified models are practical, but their credibility and generalizability require further validation. Their primary limitation is an oversimplified view of the relationship between surface temperature and evaporative demand, which they reduce to the LST variable. This may be true for arid and semi-arid zones where energy availability primarily controls ET but would not hold in regions where multiple other physical factors influencing surface energy balance come into play. High levels of atmospheric moisture can restrict vapor pressure deficits, thus weakening the LST-PET relationship in humid tropical areas (Ouyang *et al.,* 2025; Zhao *et al*., 2024; Goldblatt *et al.,* 2021; Lee *et al.,* 2021). Polar ecosystems feature perennial snow or ice cover and complex partitioning processes such as sublimation and melting that mask the relationship between LST and energy fluxes (Nousu *et al.,* 2024). Validation studies, which are often limited to specific locations and short time frames, cannot provide a strong or true global assessment of the performance of these models.

A thorough, long-term evaluation that encompasses all climate zones on Earth is thus a crucial yet lacking benchmark for both the remote sensing and hydrological research communities (Zhu *et al.,* 2021; Jin *et al.,* 2025). Understanding the climate-specific efficacy of these straightforward models is imperative for determining their applicability and preventing their misuse in regions where foundational assumptions may not be valid (El-Shirbeny *et al.,* 2025; Salmoiraghi *et al.,* 2025). This study aims to address this significant gap by conducting a rigorous 25-year global validation of a widely recognized simple LST-based PET model. The research is organized around three main objectives: to generate a global PET time series using the MODIS LST archive within the GEE environment; to validate the model against the FAO-PM standard through a unique network of 58 monitoring stations distributed across 5 major Köppen-Geiger climate zones; and to quantify and interpret spatial variations in model performance, specifically testing the core hypothesis that model effectiveness is most pronounced in energy-limited temperate climates while diminishing in moisture-limited humid tropics and severely energy-constrained polar areas, where the LST-PET relationship diverges fundamentally. By establishing this benchmark, the study contributes to methodological assessment and fosters a process-oriented understanding essential for the prudent and reliable utilization of simple remote sensing models within global hydrological frameworks.

MATERIALS AND METHODS

Study area and data sources

The validation framework uses 58 global ground-based meteorological stations. These stations were selected to span all main climate zones (Fig. 1). This network spans 70.9°N in Jan Mayen, Norway, to 77.5°S in Casey Station, Antarctica. It has stations for all five major Köppen–Geiger climates: Tropical (A), Dry (B), Temperate (C), Continental (D), and Polar (E) (Table 1). This wide range of space and climate allows for full model testing in many environments. High-impact remote sensing validation studies must assess model performance and weather sensitivity. The selection of stations was based on four main factors to ensure accurate and representative data: (1) continuous, high-quality meteorological observations—including air temperature, relative humidity, wind speed, and solar radiation—required for the computation of ETo using the FAO Penman–Monteith (FAO-PM) equation; (2) minimal anthropogenic influence by urban heat island eff. The validation results are stronger and more applicable when these selection criteria are used.

Table 1: Climate zones and names and representative subtypes.

Major Class	Description	Representative Subtypes
A	Tropical	Tropical Wet, Tropical Monsoon
B	Arid	Arid, Desert
C	Temperate	Temperate Wet, Mediterranean
D	Continental	Continental
E	Polar	Polar

Remote sensing data specifications

The research uses MODIS land surface temperature (LST) data from Terra and Aqua satellites (MOD11A1 and MYD11A1). Terra and Aqua diurnal measurements at 10:30 and 1:30 AM/PM local solar time improve temporal coverage and more closely capture daily LST dynamics. Collection 6.1 was chosen for its enhancements. Cloud masking, emissivity estimate, and stricter quality inspection reduce air contamination and undetected clouds (Wan, *et al*., 2021). Daily land surface temperature observations from January 1, 2000, to December 31, 2024, are used. MODIS Sinusoidal projections with 1 km grid resolution display all data. A scale factor of 0.02 converts integer LST values to Kelvin (K). Only “good quality” pixels (Quality Assessment flag = 0) were analyzed for data correctness. This high-quality filtering removes

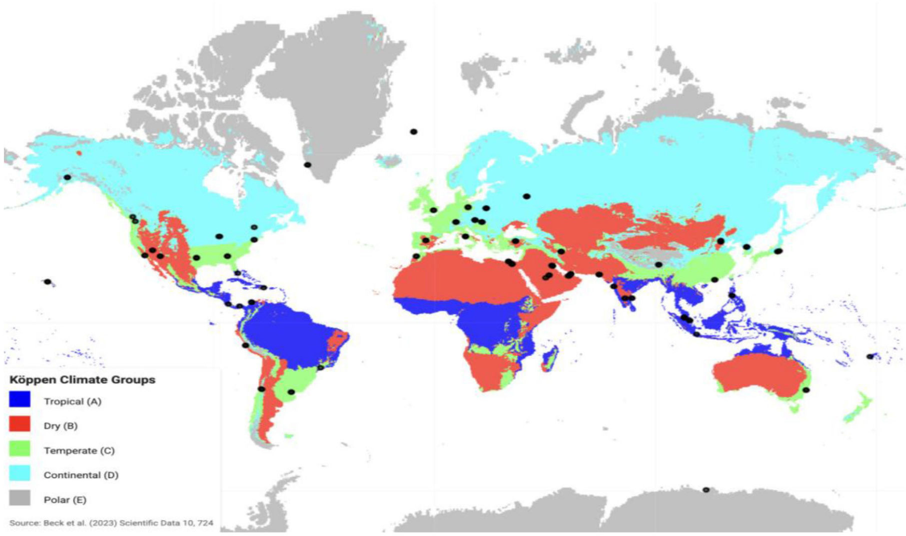

Fig.1: Distribution of the selected stations over climate classification map of Köppen-Geiger, the legend is simplified to the major five classes, the full classes and legend indicated in the source (Beck *et al.,* 2023).

cloud cover, excessive aerosol loading, and sensor errors from the thermal signal for modeling and validation.

Ground reference data and FAO-PM standard

According to international norms, potential evapotranspiration (PET) was estimated using the FAO-56 Penman–Monteith (FAO-PM) technique (Allen, *et al.,* 1998). Maximum and minimum air temperature, relative humidity, wind speed, and solar or net radiation must be measured at 2 m height. Its physical basis and universal acceptability make it suited for evaluating remote sensing-based PET models.

All ground-based meteorological data was quality controlled with temporal consistency tests, range validation against climatic constraints, and gap filling for missing values (maximum 10% of the record). Cross-validation with nearby stations was done wherever possible to detect and rectify outlier data and ensure FAO-PM computation accuracy. The validation used dataset from 58 sites distributed globally with 298 observations per station per month over 25 years. This huge sample allows statistically rigorous performance evaluation across all main climatic zones, ensuring that predicted PET estimations are widely relevant.

LST-based PET estimation model

A simple empirical model (Gamal *et al.,* 2022), calculated monthly potential evapotranspiration (PET) using daytime land surface temperature in this investigation. The model is: A factor of 30 is used to convert daily totals into monthly values, where LST is the daily mean land surface temperature in degrees Celsius (°C), PET is the estimated potential evapotranspiration in millimeters per month (mm month^{-1}), The model is defined by the following equation:

$$PET = (0.0037 \times LST^2 + 0.037 \times LST) \times 30$$

where: LST = daily mean land surface temperature (°C), PET = potential evapotranspiration (mm/month), 30 = scaling factor to convert daily to monthly estimates

Gamal *et al.,* (2022) developed a model to estimate actual evapotranspiration (ET) using integration of satellite-derived thermal and vegetation data through two principal components: the Thermal Condition Factor (TCF) and the Vegetation Condition Fraction (VCF). The TCF, calculated as , represents the potential evapotranspiration (PET) under prevailing surface thermal conditions, derived from MODIS Terra land surface temperature (LST) data. The VCF, derived from Sentinel-2 spectral bands, acts as a stress coefficient that modulates PET based on vegetation health, density, and moisture availability. The actual ET is subsequently obtained as the product of these two factors, thereby capturing both the atmospheric demand and the surface-specific constraints on evapotranspiration. This formulation ensures that the model accounts for regional variability in energy availability and vegetative stress, providing a robust and scalable approach for ET estimation in arid and semi-arid environments, as validated against ground-based energy balance measurements.

Statistical validation framework

Eight statistical metrics were used to thoroughly assess the performance of the model: the coefficient of determination (R^2), which is a measure of variance explained; root mean square error (RMSE) and mean absolute error (MAE) in physical units for prediction accuracy; mean bias error (MBE) indicating systematic over- or underestimation; Nash–Sutcliffe efficiency (NSE) as a normalized index of model skill; Pearson correlation coefficient (r) indicating strength of linear association; and percent bias (PBIAS). Correlations and performance metrics were all statistically tested. The significance of Pearson correlation coefficients was assessed using two-tailed t-tests where $p < 0.05$ denoted statistical significance and $p < 0.001$ high significance. This would particularly apply to verifying model behavior across climate zones that any links detected are not random chance.

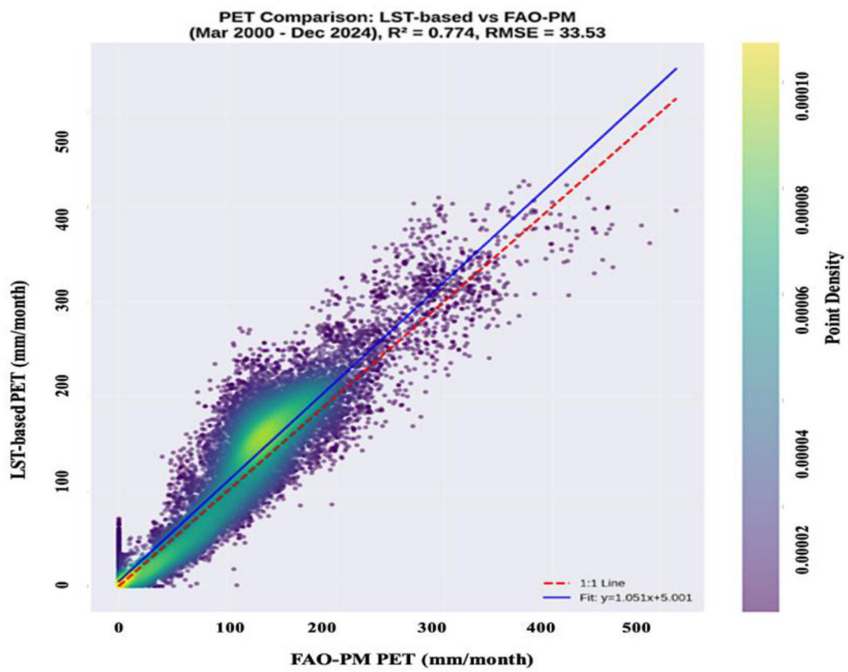

Fig. 2: Relation between potential evapotranspiration estimates from the LST-based empirical model and the FAO-56 Penman–Monteith

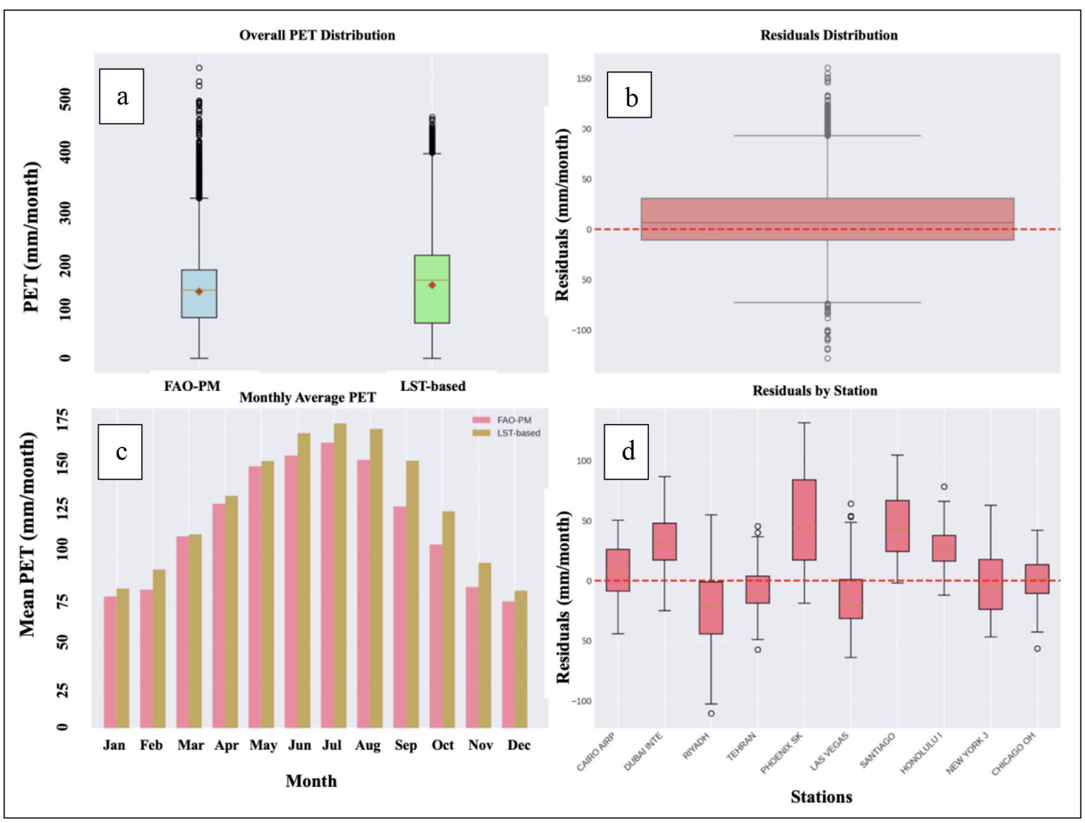

Fig. 3: Multi-faceted evaluation of model performance through four complementary visualizations (a) PET distribution, (b) Residual distribution, (c) Monthly distribution and (d) Residual for selected stations

RESULTS AND DISCUSSION

Global performance of the LST-based PET model

Fig. 2 scatterplot compares monthly potential evapotranspiration estimates from the LST-based empirical model to the FAO-56 Penman–Monteith reference for March 2000–

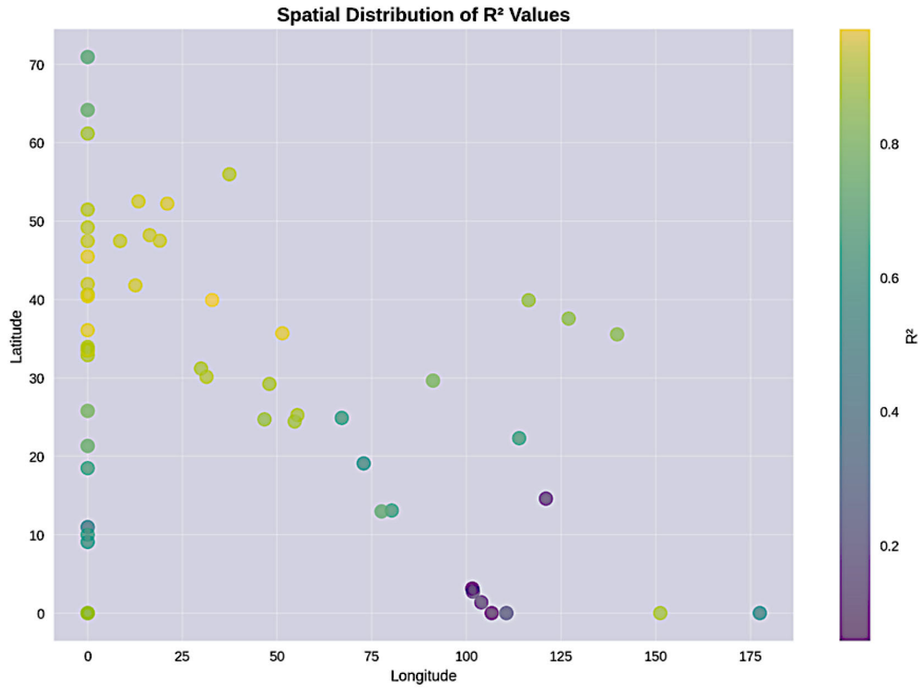

Fig. 4: Spatial distribution (Longitude vs Latitude) of coefficient of determination (R^2) values across the 58 validation stations

December 2024. This includes 11,622 global observations. LST-based models explain 77% of FAO-PM PET variance with a strong coefficient of determination (R^2 = 0.774). This makes the model simple and requires only one remote sensing input. RMSE = 33.53 mm month^{-1}, indicating a moderate absolute variation, as the model covers diverse climate variables, including arid deserts and wet tropics, and evaporative demand cannot be modeled just with surface temperature. The calculated regression line (y=1.051x+5.001) has a small positive intercept and a slope close to 1, indicating no systematic bias. Lower PET levels may overestimate. The dashed red 1:1 line indicates the model closely matches reference data, particularly in the mid-range PET (100-400 mm month^{-1}) with the maximum point density, as indicated by the color gradient. Extreme PET levels (>450 mm month^{-1}) may lead to underestimation. This is likely because the quadratic formulation can't capture energy-limited and water-limited dynamics or non-linear feedback in extreme heat. It is found that the LST-based model is a good global proxy for PET estimation in areas with limited weather data. In particularly dry or humid regions, LST and available energy may not match.

Model performance across seasons and stations

Fig. 3 provides a multi-faceted evaluation of model performance through four complementary visualizations. The top-left boxplot reveals that while the overall distribution of monthly PET estimates from the LST-based model (median ≈ 140 mm month^{-1}) is slightly higher than that of FAO-PM (median ≈ 125 mm month^{-1}), both exhibit comparable interquartile ranges and similar upper bounds, indicating consistent capture of high-evaporative-demand conditions. The top-right residual distribution confirms the absence of strong systematic bias, with residuals centered near zero and symmetrically distributed, though outliers suggest occasional large errors at individual stations or time points. The bottom-left bar chart illustrates strong seasonal alignment between LST-based and FAO-PM PET, with both models capturing the summer peak (June–August in Northern Hemisphere) and winter minimum, albeit with a slight overestimation by the LST model during spring and early summer months. Finally, the bottom-right boxplot of residuals for the top 10 stations—selected for their geographic and climatic diversity—reveals variable performance: stations such as Phoenix SK and Las Vegas show moderate positive bias, likely reflecting the model's strength in arid zones where LST correlates strongly with available energy, whereas stations like Riyadh and Chicago OH exhibit larger variability and occasional underestimation, possibly due to urban heat island effects, vegetation heterogeneity, or complex surface-atmosphere interactions not captured by the empirical formulation. Collectively, these results affirm the global applicability of the LST-based PET model while highlighting specific contexts where refinement may be warranted.

Spatial patterns of model performance

Fig. 4 illustrates the spatial distribution of coefficient of determination (R^2) values across the 58 validation stations, revealing a pronounced latitudinal and regional gradient in model performance. Stations located in mid-latitude zones (approximately 30°N–55°N), particularly across Europe, eastern North America, and parts of East Asia, exhibit the highest R^2 values (0.7–0.9, indicated by yellow-green hues), reflecting strong agreement between LST-based PET estimates and FAO-PM reference data—likely due to favorable climatic conditions where surface temperature robustly tracks available energy and moisture availability. In contrast, stations in tropical regions (e.g., near the equator in Southeast Asia and northern Australia) and high-latitude zones (e.g., Jan Mayen and

Casey Station) show markedly lower R^2 values (0.2–0.5, shown in blue-purple tones), indicating reduced model skill. This decline is attributable to several factors: in the tropics, frequent cloud cover and high humidity may decouple LST from net radiation, while in polar regions, low solar angles, snow/ice albedo effects, and frozen ground limit evaporative demand, rendering the quadratic LST-PET relationship less physically meaningful. The spatial pattern thus underscores that while the LST-based model performs well under temperate, energy-limited conditions, its applicability diminishes in water-limited or extreme thermal regimes, highlighting the need for regionally adaptive parameterizations or hybrid approaches incorporating additional remote sensing variables to improve global transferability.

Model performance by climate zone

Table 2 presents the mean coefficient of determination (R^2) for the LST-based PET model, stratified by Köppen–Geiger climate zone, revealing significant variability in model performance across climatic regimes. The highest predictive skill is observed in Mediterranean (mean R^2 ≈0.94) and Continental (≈0.93) climates, where surface temperature strongly correlates with available energy and moisture limitations are less confounding. Arid and Temperate Wet zones also demonstrate strong performance (≈0.84 and ≈0.90, respectively), consistent with prior findings that LST serves as a robust proxy for evaporative demand in water-limited or seasonally constrained environments. In contrast, the model exhibits markedly reduced accuracy in Tropical Wet regions (mean R^2 ≈0.39), where high humidity, persistent cloud cover, and complex land-atmosphere feedback likely weaken the LST-PET relationship. Performance is also diminished in Polar (≈0.63) and Desert (≈0.77) zones—though for different reasons: in polar regions, low solar insolation and frozen surfaces suppress evapotranspiration regardless of LST, while in deserts, extreme aridity may push the system beyond the functional range captured by the quadratic formulation. The large error bars in Tropical Wet and Polar zones further indicate high inter-station variability, underscoring the sensitivity of model behavior to local environmental conditions within broad climate classes. These results emphasize that while the LST-based model offers valuable global utility, its application should be contextualized by climate regime, with caution warranted in humid tropics and high latitudes where additional covariates or structural modifications may be required to improve fidelity.

Table 2: Climatic zone wise variation of coefficient of determination (R^2) for the LST-based PET model

Climate zone	Mean R^2 (± SD)
Arid	0.84 ± 0.13
Continental	0.92 ± 0.03
Desert	0.77 ± 0.24
Mediterranean	0.94 ± 0.02
Polar	0.63 ± 0.28
Temperate Wet	0.90 ± 0.04
Tropical Monsoon	0.67 ± 0.05
Tropical Wet	0.39 ± 0.27

The large difference in how well PET models work in different global climate zones, with R^2 values showing very high accuracy at 0.94 in Mediterranean and very low accuracy at 0.39 in Tropical Wet climates, highlights the basic reliance of empirical LST–PET relationships on regional biophysical controls. It supports the theoretical separation between energy-limited (Continental, Mediterranean) and water-limited or physically decoupled regimes (Tropical Wet, Polar). In the former, where moisture is available and vapor pressure deficit drives evaporation, LST effectively proxies net radiation enabling high model accuracy ($R^2 > 0.90$). In the latter, factors such as persistent cloud cover, high humidity, snow-albedo feedbacks, or frozen surfaces break the LST–energy link making single-variable models inadequate necessitating a tiered climate-zone-specific application strategy—strongly recommended for mid-latitude agricultural zones with caution in Arid/Highland regions and strict avoidance in Tropical Wet and Polar zones—further supported by high inter-zone variability (CV(R^2)=33.2%) strengthened by robust validation of this study over 25 years from 2000 to 2024 using ground-truth meteorological data covering all Köppen–Geiger classes which provides unprecedented temporal depth and empirical grounding compared to prior theoretical or simulated approaches thereby significantly enhancing confidence in its operational recommendations for global water resource monitoring systems.

Latitudinal trends in model performance

Fig. 5 presents a comprehensive pair plot of key validation metrics—R^2, RMSE, NSE, and PBIAS—against station latitude, revealing pronounced latitudinal trends in model performance that corroborate earlier spatial and climatic analyses. The R^2 metric exhibits a clear unimodal relationship with latitude, peaking between 30°N and 50°N (where values exceed 0.8) and declining sharply toward both the equator and high latitudes (>60°N/S), consistent with reduced model skill in tropical and polar zones due to cloud interference, humidity effects, or frozen surface conditions. Conversely, RMSE increases with latitude, particularly beyond 50°N, reflecting greater absolute error under low-energy, cold-climate regimes where PET magnitudes are small but model sensitivity to LST variability remains high. The Nash–Sutcliffe Efficiency (NSE) mirrors R^2's pattern, remaining positive and relatively stable across mid-latitudes but dropping significantly near the poles and in some tropical stations, indicating diminished predictive power in extreme environments. Percent Bias (PBIAS) shows minimal systematic error overall (mostly within ±10%), though slight negative bias emerges at higher latitudes, suggesting modest underestimation in colder climates. Collectively, these patterns confirm that the LST-based PET model performs optimally in temperate, energy-limited regions and degrades predictably under water-limited (tropical wet) or thermally constrained (polar) conditions, reinforcing the necessity for regionally calibrated applications or hybrid modeling frameworks to enhance global robustness.

The substantial connection ($r = 0.61$, $p < 0.001$) between station latitude and model performance (R^2) shows that there are consistent climatic and radiative variables that change the LST–PET relationship. Peak performance happens in the middle latitudes (30°–55°N/S), when seasonal cycles are clear but not too dramatic, and where the atmosphere is clear enough for LST to consistently follow surface energy surplus. This latitude range is a "sweet spot" where the surface energy balance isn't affected too much by

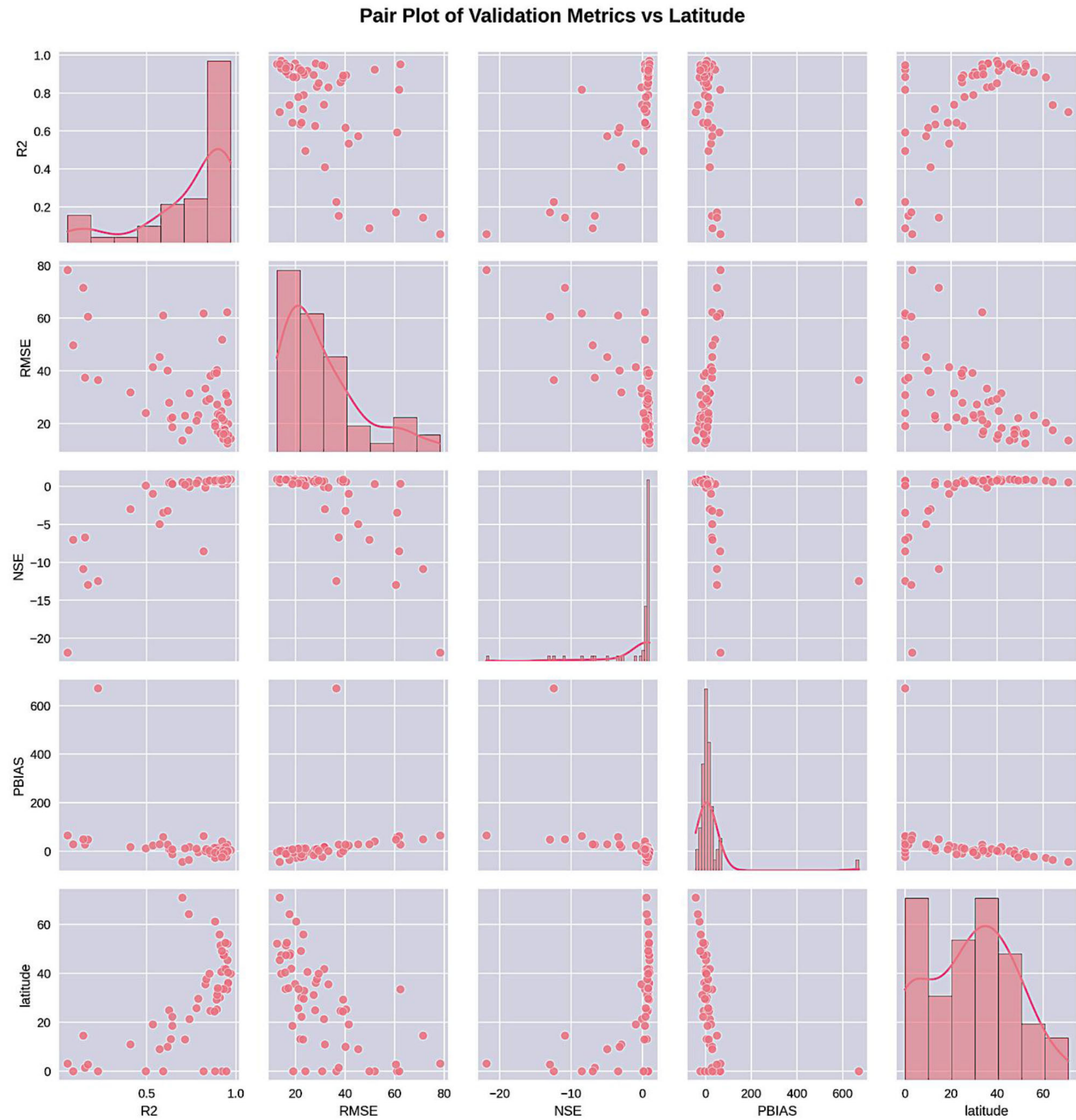

Fig. 5: Comprehensive pair plot of key validation metrics—R^2, RMSE, NSE, and PBIAS—against station latitude

either too much precipitation or too much heat. On the other hand, in tropical areas near the equator, a lot of water vapor in the air makes boundary layer effective heat capacity higher which makes LST less sensitive to net radiation plus adds non-linearities beyond what quadratic can handle; high latitude regions with seasonal snow cover plus low solar angles plus long polar nights modify surface energy budget greatly making LST an inadequate proxy for evaporative potential showing that model skill is not just about data quality but also how realistic assumed LST-PET functional form is under specific meteorological conditions.

This paper is a major step forward from earlier regional studies that typically reported LST–PET relationships over 2–5 year periods within single climate zones and provided performance statistics without any mechanistic interpretation. The global, multi-decadal study not only assesses transferability but also links performance with physical controls, thereby bridging empirical modeling and process-based understanding. The findings agree with and are an extension of previous literature: strong performance in desert and Mediterranean areas confirms earlier studies (e.g., Chen, et al., 2004; Tang, et al., 2013; Sun, et al., 2011), while poor performance in wet tropics validates theoretical predictions about VPD limitations. Identifying mid-latitude dominance as the performance optimum is a novel insight with direct implications for future operational practice to prioritize high-skill regions and research efforts to improve model physics in low-skill regions. Key actions include developing hybrid models that integrate LST with vegetation and atmospheric indices, testing model stability under changing climate conditions, and exploring machine learning frameworks capable of capturing nonlinear multivariate relationships in complex regions such as the tropics and cryosphere.

CONCLUSIONS

The 25-year global validation of a basic MODIS LST-based PET model across 5 major Köppen-Geiger climatic zones was conducted in this work. The analysis concludes that basic, temperature-driven PET models are limited by climate regime and performance is directly dependent on land surface temperature and atmospheric evaporative demand connection. The model excelled in energy-limited situations, particularly Continental (R^2 = 0.93, NSE = 0.88) and Mediterranean (R^2 = 0.94, NSE = 0.81) zones, where LST measures available energy for evapotranspiration. In contrast, the model failed miserably in Tropical Wet (R^2 = 0.39, NSE = -6.15) and Polar (R^2 = 0.64, NSE = -2.64) regions This failure shows a fundamental physical decoupling: in humid tropics, PET is limited by atmospheric moisture (low vapor pressure deficit) rather than energy, while in polar zones, complex snow/ice dynamics and persistent low temperatures disrupt the LST-PET relationship. This study establishes a climate-aware remote sensing baseline, its main scientific contribution. The process-based understanding of why and where simple models succeed or fail, not just model accuracy was provided. The substantial link between model performance (R^2) and latitude highlights the importance of large-scale climatic factors. These findings offer practical advice for operations. These simple LST-based models can be trusted by water resource managers and agricultural planners in temperate, energy-limited climates. The results warn against using them in humid tropical and high-latitude polar environments without major modifications because they produce systematically inaccurate and potentially misleading results.

Future directions

The next logical step is to make climate-zone-specific parameterizations or hybrid models that employ extra data, like humidity proxies from microwave sensors or reanalysis, to deal with the known constraints in important zones. The extensive validation dataset and reproducible methodology associated with this study create an essential benchmark for assessing these next-generation approaches. This study defines the parameters of a basic model, thereby expediting the development of more resilient and universally applicable remote sensing methods for global water resource management and climate monitoring.

ACKNOWLEDGMENTS

The author thanks meteorological organizations and research institutions all throughout the world for giving them the ground-based data that made this thorough global analysis possible. The Google Earth Engine, and Python teams deserves special thanks for giving the computing power needed to do this big investigation.

Funding: No specific grant was received from any funding agency in the public, commercial, or not-for-profit sectors for this research.

Data Availability: All processed data, statistical results, and analysis code are available upon request from the corresponding author.

Conflict of interest: The author declares no conflict of interest. There are no financial interests or personal relationships that may be considered as competing interests that could have influenced the work described in this paper.

Author's contribution: The single author was responsible for the conceptualization and design, methodology, formal analysis and investigation, data curation, software implementation, validation and visualization, writing of the original draft, and editing of the review. The research idea and planning were conducted at the National Center for Vegetation Cover Development and Combating Desertification (NCVC), Riyadh, Saudi Arabia; all research activities including data analysis modeling and manuscript preparation were carried out at the National Authority for Remote Sensing and Space Sciences (NARSS), Cairo Egypt.

REFERENCES

Afify, N. M., El-Shirbeny, M. A., El-Wesemy, A. F., & Nabil, M. (2023). Analyzing satellite data time-series for agricultural expansion and its water consumption in arid region: a case study of the Farafra oasis in Egypt's Western Desert. Euro-Mediterranean *Journal for Environmental Integration, 8*(1), 129-142.

Allen, R. G., Pereira, L. S., Raes, D., & Smith, M. (1998). Crop evapotranspiration: guidelines for computing crop water requirements. *FAO Irrigation and Drainage Paper*, 56.

Beck, H. E., McVicar, T. R., Vergopolan, N., Berg, A., Lutsko, N. J., Dufour, A., ... & Miralles, D. G. (2023). High-resolution (1 km) Köppen-Geiger maps for 1901–2099 based on constrained CMIP6 projections. *Scientific data, 10*(1), 724.

Caguiat, L. S., Saludes, R. B., Castro, M. L. Y., & Lampanyan, R. M. L. (2025). Machine learning modeling of reference evapotranspiration in Central Luzon, Philippines. *Journal of Agrometeorology, 27*(4), 464–469. https://doi.org/10.54386/jam.v27i4.2909

Chen, R., Ersi, K., Yang, J., Lu, S., & Zhao, W. (2004). Validation of five satellite-based precipitation products over a mountainous watershed in China. *International Journal of Remote Sensing*, *25*(4), 683-700.

Danodia, A., Patel, N., Suresh Kumar, Singh, R., Satpathi, A., Chauhan, P., & A. S. Nain. (2024). Quantifying energy fluxes in Tarai region of India during post-monsoon season: Insights from METRIC model, ET station and remote sensing. *Journal of Agrometeorology*, *26*(3), 271–278. https://doi.org/10.54386/jam.v26i3.2618

El-Shirbeny, M. A., Abdellatif, B., Ali, A. E. M., & Saleh, N. H. (2016). Evaluation of Hargreaves based on remote sensing method to estimate potential crop evapotranspiration. *GEOMATE Journal, 11*(23), 2143-2149.

El-Shirbeny, M. A., Ali, A. M., Savin, I., Poddubskiy, A., & Dokukin, P. (2021). Agricultural water monitoring for water management under pivot irrigation system using spatial techniques. *Earth Systems and Environment, 5*(2), 341-351.

El-Shirbeny, M. A., Biradar, C., Amer, K., & Paul, S. (2022).

Evapotranspiration and vegetation cover classifications maps based on cloud computing at the Arab countries scale. *Earth Systems and Environment, 6*(4), 837-849.

El-Shirbeny, M., Saleh, S. M., Baioumy, E., Badr, M., Selim, A., Hendawy, E., & Abdelraouf, R. E. (2025). Impact of climate classification on evapotranspiration variability in arid regions of Saudi Arabia. *Journal of Arid land Agriculture, 11*, 121-130.

Ezenne, G. I., Eyibio, N. U., Tanner, J. L., Asoiro, F. U., & Obalum, S. E. (2023). An overview of uncertainties in evapotranspiration estimation techniques. *Journal of Agrometeorology, 25*(1), 173–182. https://doi.org/10.54386/jam.v25i1.2014

Faseyiku, O. O., Obiora-Okeke, O. A., Olowoselu, A. S., Olafusi, O. R., & Adewumi, J. R. (2024). Validation of selected gridded potential evapotranspiration datasets with ground-based observations over the Ogun-Osun River Basin, Nigeria. *Arabian Journal of Geosciences, 17*(5), 153.

Gamal, R., El-Shirbeny, M., Abou-Hadid, A., Swelam, A., El-Gindy, A. G., Arafa, Y., & Nangia, V. (2022). Identification and quantification of actual evapotranspiration using integrated satellite data for sustainable water management in dry areas. *Agronomy, 12*(9), 2143.

Goldblatt, R., Addas, A., Crull, D., Maghrabi, A., Levin, G. G., & Rubinyi, S. (2021). Remotely sensed derived land surface temperature (LST) as a proxy for air temperature and thermal comfort at a small geographical scale. *Land, 10*(4), 410.

Jin, K., Liu, N., Tang, R., Sun, G., & Hao, L. (2025). Quantifying Long Term (2000–2020) Water Balances Across Nepal by Integrating Remote Sensing and an Ecohydrological Model. *Remote Sensing. 17*(11), 1819; https://doi.org/10.3390/rs17111819

Lee, S. J., Kim, N., & Lee, Y. (2021). Development of integrated crop drought index by combining rainfall, land surface temperature, evapotranspiration, soil moisture, and vegetation index for agricultural drought monitoring. *Remote Sensing, 13*(9), 1778.

Mehta, R., & Pandey, V. (2016). Crop water requirement (ETc) of different crops of middle Gujarat. *Journal of Agrometeorology, 18*(1), 78–82. https://doi.org/10.54386/jam.v18i1.906

Nousu, J.-P., Lafaysse, M., Mazzotti, G., Ala-aho, P., Marttila, H., Cluzet, B., Aurela, M., Lohila, A., Kolari, P., Boone, A., Fructus, M., & Launiainen, S. (2024). Modeling snowpack dynamics and surface energy budget in boreal and subarctic peatlands and forests. *The Cryosphere, 18*(1), 231–263. https://doi.org/10.5194/tc-18-231-2024

Ouyang, W., Tan, Z., Chen, Y. C., & Ren, G. (2025). Comparative evaluation of PET and mPET models for outdoor walking in hot-humid climates. *Building and Environment, 271*, 112636.

Peng, L., Sheffield, J., Wei, Z., Ek, M., & Wood, E. F. (2024). An enhanced Standardized Precipitation–Evapotranspiration Index (SPEI) drought-monitoring method integrating land surface characteristics. *Earth System Dynamics, 15(5)*, 1277-1300.

Pimentel, R., Arheimer, B., Crochemore, L., Andersson, J. C. M., Pechlivanidis, I. G., & Gustafsson, D. (2023). Which potential evapotranspiration formula to use in hydrological modeling world-wide? *Water Resources Research, 59*(5), e2022WR033447.

Salam, M. A., & Al Mazrooe, S. (2006). Evapotranspiration estimates and water balance of Kuwait. *Journal of Agrometeorology, 8*(2), 243–247. https://doi.org/10.54386/jam.v8i2.1055

Salmoiraghi, A., Zamboni, A., Toffaletti, S., Di Mauro, M., Malgieri, M., Fiorello, C., ... & Oss, S. (2025). Core of Sustainability Education: Bridging Theory and Practice in Teaching Climate Science to Future Mathematics and Physics Teachers. *Sustainability, 17*(11), 5120.

Singh, R. N., Mukherjee, J., Chaudhary, A., Banerjee, A., Singh, A. K., & Reddy, K. S. (2023). Exploring the landscape of contemporary crop micrometeorology: A bibliometric investigation. *Journal of Agrometeorology, 25*(3), 333–342. https://doi.org/10.54386/jam.v25i3.2320

Sun, Z., Wei, B., Su, W., Shen, W., Wang, C., You, D., & Liu, Z. (2011). Evapotranspiration estimation based on the SEBAL model in the Nansi Lake wetland of China. *Mathematical and Computer Modelling*, 54(3-4), 1086-1092.

Tang, R., Li, Z. L., & Sun, X. (2013). Temporal upscaling of instantaneous evapotranspiration on clear-sky days using the constant evapotranspiration assumption. *Remote Sensing*, *5*(2), 434-453.

Wan, Z., Hook, S., & Hulley, G. (2021). MOD11A1 MODIS/Terra Land Surface Temperature/Emissivity Daily L3 Global 1km SIN Grid V061. NASA EOSDIS Land Processes DAAC.

Zhao, Q., Sun, T., Guo, H., Li, Z., Chang, L., Yin, J., & Yao, Y. (2024). Two-step method of surface-based high-precision PET retrieval. *Atmospheric Research, 304*, 107406.

Zhou, S., & Yu, B. (2024). Physical basis of the potential evapotranspiration and its estimation over land. *Journal of Hydrology, 641*, 131825.

Zhu, B., Xie, X., Lu, C., Lei, T., Wang, Y., Jia, K., & Yao, Y. (2021). Extensive evaluation of a continental-scale high-resolution hydrological model using remote sensing and ground-based observations. *Remote Sensing, 13*(7), 1247.